Final Report: DE-FG02-03ER63646

Title: Real-time Molecular Study of Bystander Effects Using Living Cell Imaging and Nanoparticles Optics

Summary of the work Accomplished

Three specific aims were proposed in this current study. None of the originally proposed aims or the experimental design has been modified. Three investigators (each with 5% time effort) from three different laboratories are involved in this project. They are Mohan Natarajan, Ph.D. (Principal Investigator) from Department of Radiation Oncology, UTHSCSA, Nancy Xu, Ph.D. (Co-Investigator) from Department of Chemistry and Biochemistry, Old Dominion University, Virginia, and Sumathy Mohan, Ph.D. (Co-Investigator) from Department of Pathology, UTHSCSA, Texas. The budget also includes a Post-doctoral fellow at 50% time effort. In year one Specific Aim one was pursued. Aim 1: (i) To interface parallel plate flow shear system with single-molecule (SM)-single nanoparticle-single cell microscopy, (ii) To develop microprobes or nanoparticle sensors for the detection of TNF-alpha and NF-KB. In year 2 we examined (i) the proposed feed-back cycle, (ii) occurrence of radiation-induced bystander signals (iii) the contribution of TNF-alpha and NF-kB in maintaining sustained non-targeted effect and (iv) the cellular outcome (angiogenesis) as the result of persistent activation of TNF-a and NF-kB. A manuscript was drafted and currently under revision for final submission. The draft of the manuscript is attached below.

During year 1, Dr. Natarajan's group has actively worked with Dr. Xu's group in setting up the necessary research infrastructure (e.g., finding a X-ray radiation source at nearby EVMS, shipping reagents among both research groups and sharing updated research data and ideas). Dr. Natarajan visited Xu's lab twice during this period. The first visit was to make sure the X-ray radiation source and the exposure parameters are in place. At that visit a model of the flow shear system designed and routinely used by Dr. Mohan at the Department of Pathology, UTHSCSA was brought to Old Dominion University and established criteria on how to interface this flow shear system with the single living cell and single nanoparticle imaging system. In this meeting, immediate research plans were discussed in detail. The second visit is to exchange the updated research results. The summary of our current research results are given below:

(1) To interface parallel plate flow shear system with single molecule/single nanoparticle/single cell imaging system, modifications and engineering details were worked around with Old Dominion University machine shop engineers (at no cost to this project) to prepare several models of parallel plate flow shear chambers and finalized the design that would best suit to interface with the imaging systems. As described in the proposal, first the proposed experiments were carried out in the absence of flow shear system, so that the procedural details will be optimized and applied with the flow chambers. The results obtained from this study would help to distinguish the unique simulated physiology condition of flow shear system compared to static conditions.
(2) Next, to track the distribution, releasing dynamics and transport of TNF-a in real-time using the nanoparticle probes in flow shear subjected cells before and after low dose LET radiation exposures, we developed the nanoparticle sensors. To develop the nanoparticle sensors for real-time detection of TNF-a on living cell surface, we use two types of nanoparticle probes: (i) 20 nm fluorescence nanospheres and (ii) silver (Ag) nanoparticles. To study whether the antibody-linked nanoparticle

probes are still able to preserve the biological function of the antibody, we first use IgG to link with nanoparticles and study its biological activities using protein A. The reaction scheme of linking 20 nm carboxylate fluorescence nanospheres is shown in Scheme I.

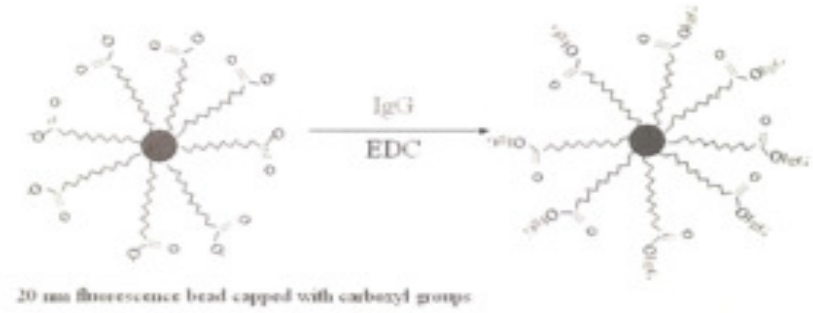

Scheme I: Covalently linking functionalized nano-bead with IgG. The caboxylate groups capped on nano-beads are linked to the primary amine groups of IgG by EDC mediated amide bond formation.

(3) Real-time images of IgG-linked nanobeads in the absence and presence of protein A are shown in Fig. 1. Individual beads are well isolated in the absence of protein A as shown in Fig. 1A. In contrast, we observed the aggregation of IgG-linked nano-beads in the presence of protein A (Figure IB). The results demonstrated that the IgG-linked nanoparticles were able to recognize protein A molecules in the solution. Also, it revealed that nanoparticle-linked IgG molecules still preserve the biological activities of IgG and can serve as a nanosensor to recognize the protein A. Thus, we will be using the similar scheme to link TNF-ct antibody with nanoparticle probes and will use such nanoprobes to detect TNF-a molecules releasing from living cells in real-time.

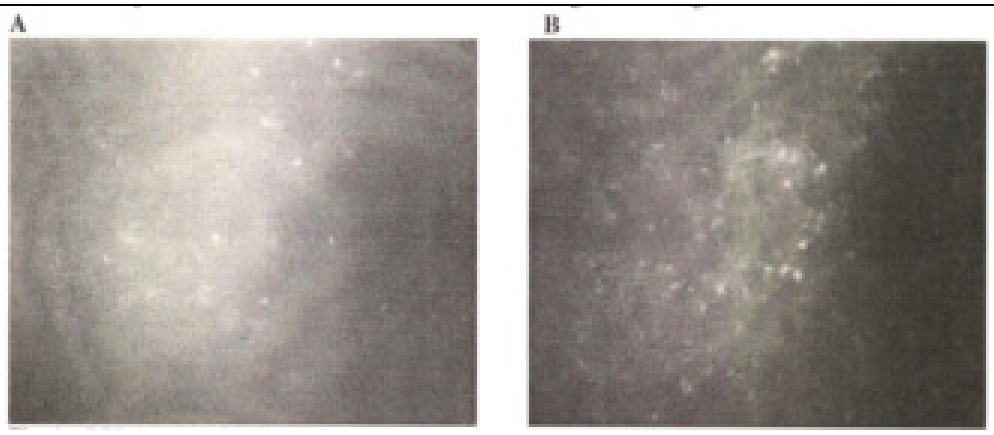

Fig. 1: CCD images of IgG-linked nanobeads: (A) in the absence of protein A; and (B) in the presence of protein A, demonstrating the biological activities of nanobead-linked IgG molecules

(4) In addition, several means to characterize the conjugation ratio of IgG with nano-beads are being developed. The calibration curve of nanobeads using UV-vis spectroscopy and the calibration curve of IgG using fluorescence spectroscopy are shown in Figure 2, indicating the possibility of using UV-vis absorbance to quantitatively measure the amount of presence of nanobeads and using fluorescence spectroscopy to quantitatively detect the amount of IgG.

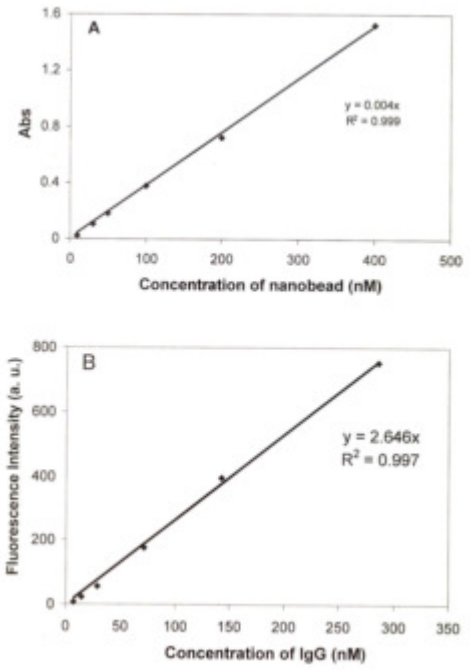

Figure 2: Calibration curves of 20 nm nano-beads(A): plots of peak absorbance at 360 nm versus nanobead concentrations, measured using UV-vis spectroscopy. Calibration curves of IgG (B): plots of peak
intensity of fluorescence emission spectra at 336 nm versus IgG concentrations. The excitation line is at 275 nm.

(5) Furthermore, we have synthesized and characterized single Ag nanoparticles as shown in Figure 3. We are exploring several reaction schemes to link Ag nanoparticles with antibodies. One of the representative reaction schemes is shown in scheme II. We are still working on the best reaction scheme to link Ag nanoparticles with antibodies and are characterizing the biological activities of Ag nanoparticle-Iinked IgG.

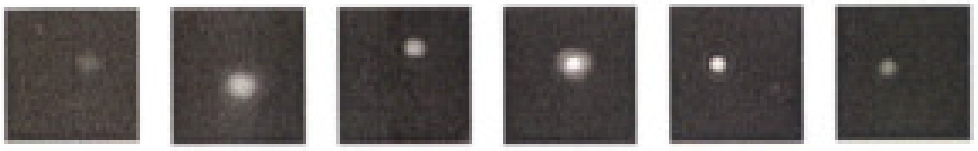

Figure 3: Images of individual Ag nanoparticles with size 10-90 nm, showing **Scheme II.** Function of Ag nanoparticles using mercaptoundecanoic acid (11-MUA) and 1-octanethiol, and covalently linking the carboxyl group of MUA with the amine group of IgG using EDC as a mediator. This allows Ag nanoparticles to be covalently linked with IgG.

(6) To characterize the biological activities of nanoparticle-linked IgG and study whether nanoparticle-Iinked IgG can recognize the receptors on living cell surface, we have cultured the endothelial cells on the microscope quartz slides and directly imaged single living cells in the microchannel. One of representative images of individual cells is shown in Fig. 4.

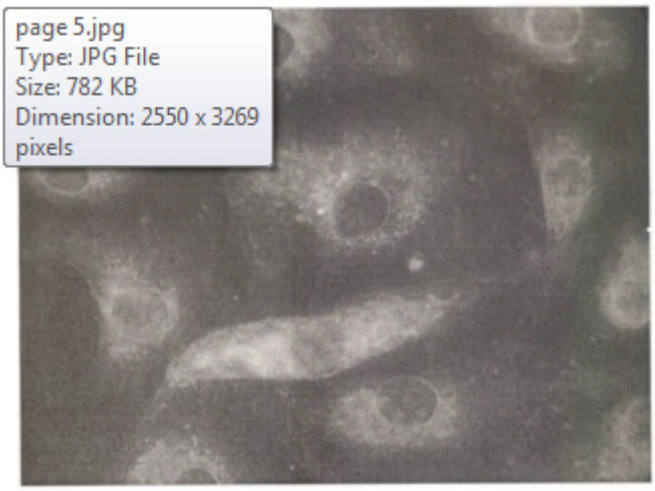

Figure 4: CCD images of single living endothelial cells (BAEC cell lines) cultured directly on a microscope slide and directly imaged in the micro-channel containing of buffer solution.

Currently applying for further funding from major grant proposal to (i) characterize the biological activities of nanoparticle-Iinked IgG and use them to detect the ligand-receptor interactions on living cell surface; (ii) expose the cells to 1 or 10 cGy and examine how the irradiated cells respond to ligand-receptor interactions; and (iii) Cells will be subjected to flow shear, exposed to 1 or l0cGy and then examined for releasing dynamics and transport of TNF-a in real time using single molecule detection microscopy. The results will be compared with one high dose of low LET radiation after exposing the cells to 10 Gy.

A Novel Mechanism of Sustained Radiation Bystander Effect: TNF-α-NF-κB positive feed-back signaling maintains the memory of radiation insult that is responsible for tumor-derived angiogenesis

Hui Yu[1], Sumathy Mohan[3], Natarajan Aravindan[4,] Mohan Natarajan[1,2]

Departments of [1]Radiology, [2]Medicine and [3]Pathology, University of Texas Health Science Center, San Antonio, Texas.
[4]Department of Radiation Oncology, University of Oklahoma Health Sciences Center, Oklahoma City, Oklahoma

Key Words: Breast cancer, Non-targeted effect, low LET radiation, TNF-alpha, NF-kappa B, Feed back cycle and MCF-7 cells.

Running Title: Mechanism of sustained radiation insult

Address for Communication:

Mohan Natarajan, Ph.D

Professor

Department of Medicine, School of Medicine

University of Texas Health Science Center

7703 Floyd Curl Drive

San Antonio Texas, 78229.

Phone: (210) 567-5654

Fax: (210) 567-0379

E-mail: natarajan@uthscsa.edu

Abstract:

Although it is well established, radiation-induced bystander effect is still a subject of considerable discussion and controversy on how these signals are amplified enough to realistically cause an effect. It is highly unlikely that an independent factor or a unidirectional signaling pathway, as reported in most of the radiation-induced bystander studies, could address this concern. We have shown in MCF-7 cells, exposed to a total dose of 2 or 10 Gy at a dose rate of 1.03 Gy/min, a rapid activation of NF-kB (4.7±0.6-folds at 3 h), which in turn induces the expression and secretion of soluble TNF-a (1.9±0.08-fold). Secreted soluble TNF-a then stimulates a second phase NF-kB activation through an autocrine mechanism. Recycling of these two proteins through a positive feedback loop, in the irradiated cells, amplify and maintain a memory of the initial insult for an extended period. Medium transfer experiments revealed that the secreted TNF-a concurrently initiates an identical TNF-a-NF-kB feed back cycle in the bystander cells through a paracrine mechanism and thus extend the initial impact in the non-targeted cells. Co-culturing of irradiated MCF-7 cells with the endothelial cells results in NF-kB-mediated angiogenesis showing evidence that inter-cellular signaling through this positive feed back signaling pathway could cause an effect at cellular level. This study shows evidence that radiation-triggered signals are sustained through a positive-feed back loop, amplified and transmitted to the surrounding micro-environmental niche through a bystander mechanism, resulting in propagation and radial expansion of those signals in non-targeted cells, that it could cause a protracted radiation effect.

Introduction:

Radiation-induced bystander effect was re-emphasized in 1992 by Nagasawa and John little long after it was first reported in 1947 by Kotval and Gray. Since then the mode of communication was argued as a cross-talk between cells through gap-junction mechanism () or through extra-cellular matrix (). Follow-up investigative reports including our own findings raised the possibilities of series of soluble macromolecular factors, which are commonly functions as the mediators in intracellular signaling pathways for the communication between the targeted to the non-targeted cells (). Those mediators, though proven beyond doubt that (i) they are significantly induced upon radiation exposure of cells *in vitro*, (ii) cross through cellular membrane and (iii) cause structural and functional alteration in the neighboring cells that are protected from irradiation, their involvement in acute or long-term outcome of radiation response is not completely understood. The response(s) caused by the insult of radiation that result in bystander effect need to be kept in the memory of cells (long-lived) and the resulting effect should be a domino effect. In the absence of these two phenomenon, the alterations caused in the non-targeted cells will be un-noticed due to predisposal of the cells to apoptosis or other mode of cell death and eliminated from the cellular milieu. The communication will result in traveling a short distance. The *in vivo* abscopal study () or *in vitro* tissue model () it has been shown that radiation induced response travel longer distance and cause acute and late radiation effects. Therefore, in this study we investigated and reported a novel mechanism that addresses how the signals triggered by radiation are kept in a long-term memory and communicated to adjacent or distant cells to cause a domino-effect and late radiation response.

Materials and Methods:

***Cell Culture**:* Estrogen receptor positive human adenocarcinoma (MCF-7) breast cancer cells (obtained from American Type Culture Collection, Bethesda, MD) and primary Bovine aortic endothelial cells (BAEC; Clonetics /BioWhittaker, San Diego, CA) were maintained in Dulbecco's Modified Eagle medium (DMEM; Life Tech., Grand Island, NY) and MCDB-131 medium (Sigma, St. Louis, MO), respectively as described earlier (). The murine L929 fibroblast cell line (ATCC), used for TNF-α cytotoxicity bioassay as the target cells (Sugarman BJ, 1985), were grown in supplemented Eagles minimum essential medium (EMEM; Sigma Chemical Co., St. Louis, MO) containing 2 mM L-glutamine, 10.2 I.U/ml penicillin, 10.2 µg/ml streptomycin, 10 mM HEPES and 10% heat-inactivated fetal bovine serum. The cells were grown in a 95% air/5% CO_2 humidified incubator. For all the experiments the cells were serum-starved by incubating at 2% serum containing complete growth medium for at least 16 h unless otherwise specified. Cell viability was determined by the trypan blue dye exclusion method (1).

Exposure to ionizing radiation: For the selected doses of low-LET radiation exposures, the cells were removed from 37°C incubator and exposed to 2 or 10 Gy of ^{137}Cs γ-rays at a dose rate of 1.29 Gy/min (Atomic Energy of Canada Ltd GammaCell-40 Irradiator) at room temperature (22°C). Immediately after exposures, the cultures were returned to the 37°C incubator and harvested at selected time points specified for each experiment. Mock-irradiated control cells (0 Gy) were treated identically except the cells were kept outside exposure chamber.

stored at -80^{o}C.

Electrophoretic Mobility Shift Analysis (EMSA): EMSA analysis in the nuclear proteins were performed according to the method described in our earlier studies (Mohan *et al. 2007)* using a double-stranded oligonucleotide (5' -AGT TGA GGG GAC TTT CCC AGG C-3'; Promega,

Madison, WI) containing a tandem repeat of the consensus sequence 5'-GGG GAC TTT CC-3' end-labeled with T_4 polynucleotide kinase. To test the specificity of the NF-kB DNA-binding activity, a competition assay was performed. The nuclear extract (2 µg of protein) was pre-incubated with 5 or 50 molar excess of unlabeled homologous NF-κB oligonucleotide for 5 min on ice, followed by addition of γ-^{32}P-labeled NF-κB probe. The total amount of NF-κB activation was determined by quantitative analysis of the autoradiogram using 'NIH Image J' software.

TNF-a Bioassay: The activity of TNF-a was determined by a cell-based cytotoxic bioassay (Sugarman, 1985). The murine L929 fibroblast cells (4 x 10^4 cells/well) were seeded into flat bottom 96-well microtiter plate in 100 ul of complete EMEM medium and incubated overnight at 37^{o}C air/CO_2 incubator. Platting density was optimized and care was taken to keep the cell density equal for all the wells seeded. The cells were then equilibrated with fresh growth medium containing 2% serum for at least 2.5 h. The medium was replaced with 50 µl of test samples (i.e. conditional medium from irradiated and mock-irradiated MCF-7 cells) and 50 ul of actinomycin D (8 µg/ml). The micro-titer plates were further incubated for 16 h and then added with 10 ul of proliferation assay reagent WST-1 (Roche Diagnostics, Indianapolis, IN) and incubated for additional 2 h. To generate standard curve of 1pg to 1µg, recombinant human TNF-α (R&D Systems, Minneapolis, MN) was used The absorbance at 460 nm was measured against the background control as blank using a Microplate reader (MR-5000, DYNEX, Chantilly, VA). The mean ± SD of the percentage of L929 cytotoxicity was calculated by data obtained from quadruplicate wells.

Transient Transfection and NF-κB-dependent reporter assays: The pTAL-Luc and pNF-κB-Luc plasmids (containing four putative binding sites for NF-κB; Mercury pathway profiling luciferase system, Clontech Laboratories, Palo Alto, CA) were used at a concentration of 1µg/µl

for transfection. MCF-7 cells seeded in 60 mm culture dishes at a density of 1 x 10^5 cells/plate were allowed to grow up to 70% confluent and equilibrated with fresh growth medium containing 2% serum. Transfection was performed using Effectene^{TM} transfection reagent (Qiagen) as described earlier (Mohan et al, 2007; 8.2 Ghz paper). The transfected cells were incubated for 8 h at 37^{o}C. The medium containing transfection mixture was then replaced with fresh growth medium containing 2% FBS and incubator for 2.5 h. At that time, the cells were exposed to selected doses of radiation or sham-exposed. The cells were then incubated for additional 8, 24 and 48 h, harvested, and assayed for luciferase activity. To monitor the differential transfection efficiency, the cells were co-transfected with an expression vector containing enhanced green fluorescent protein (pEGFP-Luc; Clontech). Before lysis, an aliquot of cells were evaluated for transfection efficiency by flow cytometry using the FACScan and CellQuest 3.3 software package (Becton-Dickinson, San Jose, CA). The luciferase activity in 20 µl cell extract was determined using the Dual Luciferase Assay and Detection System following the manufacturer's protocol (Promega, Madison, WI).

Co-culture System: For indirect co-culture, MCF-7 were cultured in apical compartments of cell culture inserts (Pore size: 0.45 µm, growth area: 4.2 cm^2, Falcon-BD Bioscience, Franklin Lakes, NJ, USA) with endothelium cells in the basal compartment of 6-well plates (growth area: 9.6 cm^2). Because MCF-7 had shorter doubling time than endothelium cells, different numbers of MCF-7 (2 x 10^5 cells) and endothelium cells (5 x 10^4 cells) were seeded. The semipermeable membrane of the insert allows the diffusion of secreted factors but prevents the cells transporting from one chamber to the other. Complete MCDB growth medium were shared by both the MCF-7 and endothelial cells which were grown completely separated. At 16 hours after cells were seeded, the inserts containing MCF-7 cells were placed on a separate 6-well plate (exposure

plate) containing MCDB medium with reduced serum (2% FBS) and either mock irradiated or exposed to selected doses of radiation. Immediately after exposure, the inserts were taken out of the exposure plate and placed on the 6-well plate containing endothelial cells (bottom chamber). After 16 hours, the expression of angiogenic growth factor receptors was measured in the co-cultured endothelial cells. Secretion of complementary growth factors from the MCF-7 cells was measured in the culture medium.

Western Bloting: To enrich the proteins in the conditioned medium, the disposable Centrifugal Filter Devices containing anisotropic membranes (Millipore, Billerica, MA) were used. To concentrate VEGF and bFGF in the medium, filter devices containing the molecular weight cut off of 30,000 kDa (YM-10) and 10,000 kDa (YM-3), respectively were used. Cytoplasmic proteins from treated or exposed MCF-7 cells were extracted in 100 µl of cold RIPA buffer (25 mM Tris-HCl pH 7.6, 150 mM NaCl, 1% NP-40, 1% sodium deoxycholate, and 0.1% SDS) containing a cocktail of protease and phosphatase inhibitors [1 mM of protease inhibitor, (PI; Sigma) and 1 mM of Phenylmethanesulfonyl fluoride (PMSF, Sigma)] following the method described in our earlier publication (Mohan *et al. 2007).*

Equal amount of protein samples from the cytoplasmic extract or from the concentrated medium (50 or 100 µg) were analyzed for VEGF and b-FGF expression using anti-VEGF or anti-bFGF (1:1,000 dilution; Abcam, Cambridge, MA). To determine the expression of reciprocal receptor expression in the endothelial cells that were co-cultured with MCF-7 cells, VEGFR2 and FGFR1 were examined using anti-VEGFR2 and anti-FGFR1 antibodies (1:1,000 dilution; Abcam, Cambridge, MA) as primary antibodies and a 1:10,000 dilution of horseradish peroxidase-conjugated secondary antibody (Santa Cruz Biotechnology, CA). The autoradiograms were scanned (Agfa company ?) and the protein expression was quantified using Adobe

Photoshop Image-J software (Adobe, San Jose, CA). To monitor equal loading of protein, the samples were probed for β-actin or α-tubulin expression.

Tube formation assay in 3D matrigel matrix: To determine indirect effect of radiation on tubule formation, co-culture system were used. First, MCF-7 cells (1×10^4 cells/well) in complete MCDB medium (10% FBS) were seeded in the compartment of the cell culture inserts, which were in the exposure plates overnight. Four hours before radiation exposure, the complete MCDB medium were replaced by plain MCDB medium in the MCF-7 cells, then were either mock irradiated or exposed to radiation. After radiation exposure, another 24-well plate was coated with 300 µl of Matrigel per well to the growth surface and incubate coated surface for 1 h at 37°C to allow the gel to solidify. Endothelial cells (1×10^4 cells/well) in plain MCDB medium were then seeded in coated 24-well plate in the presence or absence of angiogenesis inducers (VEGF and bFGF, 3 ng/mL) or inhibitors (NF-κB inhibitor, 10 µM). After 3 hours, cell culture inserts with MCF-7 cells were transferred to the endothelium cells plates. The tube formations were found 8-10 hours later. Three random fields were viewed in triplicate wells for each test condition under high power Nikon ECLIPSE TE 2000-U microscope linked to a computer with Adobe Photoshop 7 software. Quantification of tubule formation was carried out by counting the number of tubule junction in the total area covered by tubules in each field using image analysis software Photoshop version 7.0.

Statistical Design and Methodologies: The proposed experiments were performed a minimum of three times in two sets. Data were expressed as mean ± SD. Statistical analyses were performed using paired and unpaired Student's t-test to determine significant changes between test samples and controls. Paired data were used with repeated measures of analysis of variance. Statistical significance was defined as $p < 0.05$.

Results:

Positive feedback loop sustains initial radiation insult caused by a single exposure.

Irradiated cells secrete functionally active soluble TNF-α into the culture medium: To study whether the pro-inflammatory cytokine TNF-α is the mediator in the radiation-triggered autocrine feedback cycle, radiation-induced functionally active TNF-α expression and subsequent secretion into the culture medium were measured. MCF-7 cells either mock irradiated or exposed to 2 or 10 Gy were harvested at 8 and 24 hours. Secreted TNF-α levels were determined by cell-based cytotoxic bioassay using L929 fibroblast cells as the target cells. Since not all L929 fibroblast cells are TNF-α sensitive, and those that are sensitive may vary in their degree of sensitivity (Hogan and Vogan, 2000), cellular susceptibility to TNF-α was monitored using serial dilution of recombinant human TNF-α (rhTNF-α) by WST cytotoxicity assay () prior to the experiments. The secreted TNF-α levels in the culture supernatant from cells exposed to 2 Gy and harvested at 8 hours showed a 1.9 ± 0.08-fold increase compared to mock-irradiated control. The amount of secreted TNF-α remained at the same level even after 24 hours post radiation (Figure 1). TNF-α bioactivity in culture supernatant of the cells exposed to 10 Gy showed only a moderate increase. The levels were 1.4 ± 0.1- and 1.2 ± 0.2 -folds at 8 and 24 h, respectively. Culture supernatant incubated with TNF-α antibody prior to bioactive assay confirmed the specificity of the induced TNF-α levels. The levels of secreted TNF-α in the supernatant form activated normal human monocytes (Mono Mac 6; MM6) by stimulating with 1 ng/ml of LPS and harvested at 24 h were used as assay control.

Transactivation of TNF-α in the irradiated cells is mediated by radiation-induced activation of NF-κB: Radiation triggers NF-κB activity in MCF-7 cells. MCF-7 cells were exposed to

radiation to a total dose of 2 or 10 Gy. Irradiated cells were incubated for 15 minutes or 3 h. NF-κB DNA-binding activity in the nuclear extracts was examined by electrophoretic mobility shift assay (EMSA). The cells were predominantly viable at the time points examined for EMSA after exposure to 2 or 10 Gy. A representative autoradiogram showing the gel pattern is presented in Figure 2. A detectable constitutive level of NF-κB DNA binding activity was observed in the untreated mock-irradiated control (lane 1). The samples from cells exposed to 2 Gy and examined at 15 minutes show a significant increase above the constitutive level (Figure 2 A; lane 2). As the exposure increased to 10 Gy the induced levels of NF-κB activity at 15 minutes was slightly reduced (lane 3) than that of 2 Gy exposed cells. The levels of NF-κB activity determined by densitometric quantitation of specific bands showed 4.0 ± 0.3 and 3.4 ± 0.8-folds higher than the mock-irradiated control (Figure 2 C) after 2 and 10 Gy, respectively. At 3h post-exposure, the activation of NF-κB further increased and reached its maximum (4.8 ± 0.6-folds) after 2 Gy exposure (Figure 1, lane 5), but remained at the same level as seen at 15 minutes after 10 Gy exposure (3.3 ± 0.3-folds). Competitive binding assay performed in the nuclear extract from cells exposed to 2 Gy and harvested at 3 h confirmed the specificity of the NF-κB-DNA binding activity (Figure 2B, lane 1). NF-κB DNA-binding activity was competitively reduced to 85 % and 30 % by the addition of 2.5 and 25 molar excess of homologous unlabeled NF-κB specific-double stranded oligonucleotide probe, respectively (Figure 2B, lanes 4 and 5). The non-homologous competitor AP-1 did not inhibit the NF-κB DNA binding activity (Figure 2B, lane 3).

Next, to determine whether radiation triggered DNA binding activity of NF-κB is functionally viable and could up-regulate the κB-dependent gene expression, transient transfection assays were performed. MCF-7 cells were transiently transfected with pNF-κB -Luc

plasmid construct that expresses the luciferase reporter gene in an NF-κB-dependent manner. It contains four tandem copies of the NF-κB consensus sequence fused to a TATA-like promoter region of herpes simplex virus's thymidine kinase promoter. Functionally active NF-κB specifically binds to the promoter and activates transcription allowing reporter gene to be expressed. Cells transfected with pTAL-Luc construct were used as a negative control as well as to measure the background. A promoter/enhancer less pGL3-basic vector was used as a transfection control. Absence of luciferase activity in cells transfected with pGL3-basic vector and then irradiated confirmed the absence of gene expression due to transfection procedure using cationic lipid reagents. Minimal luciferase activity observed in cells transfected with the pTAL-Luc control vector was used to determine the non-specific luciferase activity. To ensure that the luciferase assay was within the linear range, the standard curve of light-units versus relative enzyme concentration was obtained by making serial dilutions of recombinant luciferase (Promega, Madison, WI) in 1 x lysis buffer with 1 mg/ml BSA. Transfection efficiency was normalized by determining the relative optical density values of *Renilla* luciferase activity. The induced levels in cells transfected with pNF-κB-Luc plasmid construct were then calculated by comparing the levels seen in mock-irradiated cells. Compared to mock irradiated control, the luciferase activity in cells exposed to 2 Gy was slightly increased at 8h (1.3± 0.07-fold), the earliest time point examined. The activity was increased to its maximal level at 24 h (2.3 ± 0.06-fold) and reduced at 48 h (1.5 ± 0.09-fold) (Figure 3). Cells exposed to 10 Gy showed only a slight increase at 24 h (1.4 ± 0.07- fold) and remained at the constitutive levels at 8 and 48 h. Similarly, cells transfected with pTAL-Luc control vector remained at the basal levels at all time points examined. These results clearly indicated that induction of NF-κB DNA binding activity

seen after 2Gy was functionally active and therefore could initiate activation of NF-κB-dependent gene transcription.

To determine the causal relationship of NF-κB activation and extracellular TNF-α synthesis in the culture supernatant, alterations in the secreted levels of TNF-α was measured after blocking NF-κB activation. MCF-7 cells were incubated with NF-κB inhibitor isoheleninm at a final concentration of 10μM (Calbiochem, NJ) for 6 hours (Figure 4A). Isohelenin is a cell-permeable sesquiterpene lactone with anti-inflammatory properties and acts as a highly specific, potent, and irreversible inhibitor of NF-κB activation by preventing IκB degradation (Figure 4B). Intact IκB remain bound to NF-κB and prevent the active NF-κB to translocate into the nucleus. When NF-κB-dependent transactivation was inhibited, the levels of secreted TNF-α was decreased about 50% and 40% in cells exposed to 2 Gy and harvested at 8 and 24 h, respectively.

TNF-a autocrine pathway is responsible for second phase activation of NF-kB in irradiated cells: First, we examined whether the rapid activation of NF-κB in the irradiated cells was transient or persistent. MCF-7 cells were exposed to 2 Gy, re-incubated and harvested at 15 min, 3h, 16h, 24h, 36h and 48h for EMSA analysis. There was a persistent activation of NF-kB after radiation exposure. However, radiation-induced activation of NF-kB appeared to be bi-phasic. The rapid activation of NF-kB at 15 minutes after radiation exposure (5.4-fold ± 0.4) was found to be maximum at 3 h showing a 7.2-fold ± 1.4, compared to mock irradiated control. The DNA-binding activity of NF-kB started reducing and reached to the basal level at 16 h. At 24 h after irradiation, the DNA-binding activity again increased as a second phase activation (3.8-fold ± 1.1) and reached a second maximum at 36h (4.85-fold ± 0.3). The activity started decreasing after 48 h (1.9-fold ± 1.3), the latest time point examined (Figure 5). Since IR-induced soluble

TNF-a levels were elevated in the culture supernatant of MCF-7 cells, and since ectopically added recombinant TNF-a is a known inducer of NF-kB, next we examined whether the secreted TNF-α, as an autocrine inducer, is responsible for the second phase activation of NF-κB signaling. MCF-7 cells were incubated with TNF-α neutralizing antibody at 8, 12 and 16 h after radiation. Pre-immune IgG was used as the antibody control. In the presence of TNF-α antibody, the 2nd phase activation of NF-κB seen at 36 h was significantly inhibited by 56.1%, 69.5% and 71.5 % in cells in which TNF-a antibody was added at 8, 12 and 16 h, respectively. Significant reduction in 2nd phase activation of NF-kB confirming that the secreted TNF-α was responsible for the stimulation of NF-κB at later time points (Figure 6).

Overall the findings from the first part of the study revealed that: **(a)** NF-κB DNA-binding activity is triggered in MCF-7 cells after exposure to radiation at clinically relevant doses. **(b)** The induced NF-κB activation is functionally viable that it could transactivate the κB-dependent downstream genes. **(c)** The radiation-induced activation of NF-κB is bi-phasic, showing 1st maximum level at 3h and the 2nd peak at 36 h. **(d)** Radiation at clinical doses could stimulate the expression and secretion of TNF-α into the culture medium. **(e)** TNF-α secretion was NF-κB dependent and the radiation-induced rapid activation of NF-κB at 3 h is responsible for the transactivation of TNF-α gene expression. **(f)** TNF-α mediates the second phase activation of NF-κB through autocrine mechanism in the irradiated cells.

Extension of positive feedback loop to the bystander neighboring cells:

To determine the mechanism of TNF-α mediated bystander effect in the un-irradiated neighboring cells: To study whether TNF-α regulates NF-κB activation in the bystander cells**,** medium from MCF-7 cells that are irradiated and incubated for 24 hours was transferred into the cultures of non-irradiated MCF-7 cells. We found that the DNA-binding activity of NF-κB was

increased to 7.2 ± 1.4-fold in the non-irradiated cells as early as 15 minutes compared to the mock-irradiated control (Figure 2.8 A and B). The activation was persistent up to 24 h, the latest time point studied. Similarly the luciferase activity also corroborated the results of DNA binding activity showing an increased functional activation of NF-κB in the un-irradiated bystander cells (Figure 2.8 C) upon transfer of medium from the irradiated cells. To investigate the possibility that the presence of secreted TNF-α in the medium from the irradiated cells may be responsible for the initiation of NF-κB signaling in the non-irradiated cells, we transferred the conditional medium from the irradiated cells after blocking TNF-α by incubating with TNF-α neutralizing antibody for the last 8 hours (i.e. 16 hours after irradiation) prior to adding to the non-irradiated MCF-7 cells. Measure of functional assay showed a ____ % blockade in the NF-kB-luciferase activity in the non-irradiated MCF-7 cells at 3 h after the addition of the conditional medium (Figure 2.8 D). Interestingly, normal endothelial cells that are co-cultured with irradiated MCF-7 cells showed similar response. There was an increased NF-kB activity in the non-irradiated endothelial cells when co-cultured with irradiated MCF-7 cells, which is significantly inhibited when the medium was incubated with TNF-a neutralizing antibody.

Cells transiently transfected with TNF-a promoter containing 4 tandem repeats of NF-kB binding site when incubated with irradiated MCF-7 cells showed an increased induction of TNF-a promoter activity. The results confirmed the occurrence of second round of NF-kB-TNF-a feed back cycle in the non-irradiated bystander endothelial cells (Figure).

To further confirm that NF-□B governs the transcriptional activation of TNF-□ gene promoter, cells were transiently transfected (using Effecten^{TM} reagent) with TNF-□ promoter constructs containing functional wild type □B binding site or mutant □B binding sites associated with chloramphenicol acetyl transferase reporter gene (obtained from Dr. Patrick A Baeuerle, Tularik

Inc., San Francisco, CA). The cells were mock-transfected or transfected with either wild type construct or mutant construct. The transfected cells were exposed to 2 Gy and assayed for CAT activity at 24 h post exposure by thin layer chromatography. Actin promoter associated with CAT was used as an internal control. Assay control containing 1U of chloramphenicolacetyl transferase treated identically was included for each assay. CAT activity was induced in wild type TNF□□ promoter in response to 2 Gy exposure, but not in cells transfected with mutant construct compared. The results revealed NF-□B-dependent TNF□□ promoter activation ***(Figure 12).***

Communication of irradiated MCF-7 cells to non irradiated endothelial cells mediated by TNF-a-NF-kB feedback loop initiates angiogenic signaling:

Angiogenic growth factor induction by MCF-7 cells: Tumors require blood supply to survive, grow and metastasize, which involves the process of angiogenic signaling for new blood vessel growth into a growing tumor mass. Secreted angiogenic growth factors functions as the mitogen for micro- and macro-vascular endothelial cells. To test the hypothesis that the surviving tumor cells after radiation exposure could enhance the expression and secretion of angiogenic growth factors for their maintenance and re-growth, the intra-cellular and secreted levels of key angiogenic growth factors, VEGF and FGF-2 were examined in MCF-7 cells exposed to 2 Gy and harvested at 16 h. The cytoplasmic and secreted levels of VEGF were 4.5±0.6 and 3.4±0.7-folds, respectively (Figure). Cells incubated with VEGF peptide1µg/ml completely blocked the radiation-induced VEGF expression confirming the specificity. Similarly, the cytoplasmic and secreted levels of FGF-2 were increased in cells exposed to 2Gy. The levels were 3.7± 0.8 and 2.6±0.9-folds in the cytoplasmic extract and in the culture supernatant, respectively. Cells incubated with NF-kB inhibitor isohelenin (10 µM), one hour prior to radiation, decreased the intracellular expression and secreted angiogenic growth factors, confirming that the radiation-

triggered NF-kB feed back cycle is responsible for the induction of angiogenic growth factors (Figure).

Angiogenic receptor expression in the co-cultured non-irradiated endothelial cells:

Endothelial cells were co-cultured with MCF-7 cells exposed to 2 Gy and harvested at 16h. Expression of angiogenic receptors was examined in the endothelial cells. Endothelial cells treated with recombinant VEGF (rhVEGF, 50 ng/ml) or o.1 μM PMA were used as positive controls for VEGFR2 and FGFR1 expression, respectively. The expression levels of VEGFR2 and FGFR1 were increased by 2.9±0.9- and 3,8±0.3-folds, respectively.

Next we examined in vitro tube formation of endothelial cells. Co-culture system of endothelial and MCF-7 cells were used. Cells treated with rhVEGF were used as a positive control. Increased tube formation was observed in cells co-cultured with MCF-7 cells. The network was further increased when the endothelial cells are co-cultured with MCF-7 cells that are exposed to 2 Gy. NF-kB inhibitor isohelenin (10μM) significantly inhibited the number of junction confirming the radiation-induced NF-kB is responsible for initiation of angiogenic network formation.

Results:

Radiation triggers NF-κB DNA binding activity in ER (+) MCF-7 cells: Since the radiation-induced cascade of events that result in sustained bystander effect is proposed to be initiated by the activation and the nuclear translocation of NF-κB, we first examined the DNA-binding activity of NF-κB in the nuclear extracts of cells exposed to low LET radiation. MCF-7 cells were exposed to ^{137}Cs gamma radiation to a total dose of 2 or 10 Gy. Irradiated cells were incubated for 15 minutes and 3 h. NF-κB DNA-binding activity in the nuclear extracts was examined by electrophoresis mobility shift assay (EMSA). The cells were predominantly viable

at the time points examined for EMSA after exposure to 2 or 10 Gy. A representative autoradiogram showing the gel pattern is presented in Figure 1. A detectable constitutive level of NF-κB DNA binding activity was observed in the untreated mock-irradiated control (lane 1). The samples from cells exposed to 2 Gy and examined at 15 minutes show a significant increase above the constitutive level (Figure 1 A; lane 2). As the exposure increased to 10 Gy the induced levels of NF-κB activity at 15 minutes was slightly reduced (lane 3) than that of 2 Gy exposed cells. The levels of NF-kB activity determined by densitometric quantitation of specific bands showed 4.0 ± 0.3 and 3.4 ± 0.8-folds higher than the mock-irradiated control (Figure 1 C) after 2 and 10 Gy, respectively. At 3h post-exposure, the activation of NF-κB further increased and reached its maximum (4.8 ± 0.6-folds) after 2 Gy exposure (Figure 1, lane 5), but remained at the same level after 10 Gy exposure (3.3 ± 0.3-folds).

To confirm that the shifted bands seen in EMSA analysis was due to the specific binding of NF-kB to its sequence-specific oligonucleotides, and to confirm that we were restricting the quantitative analysis to the NF-κB-specific region of the gel, a competition binding assay was performed. Nuclear extracts obtained from cells exposed to 2 Gy and harvested at 3 h post-exposure (Figure 1 B, lane 1) were pre-incubated in the presence or absence of homologous unlabeled (cold) oligonucleotide competitor identical to the NF-κB specific probe. In the presence of excess cold competitior, only a few binding sites of NF-κB will be presented to the γ-^{32}P-labeled oligonucleotide, thereby reducing the intensity of the resulting band in the gel electrophoresis. As shown in Figure 1B, the NF-κB DNA-binding activity was competitively reduced to 85 % and 30 % by the addition of 2.5 and 25 molar excess of homologous unlabeled NF-κB specific-double stranded oligonucleotide probe, respectively (lanes 4 and 5). The non-homologous competitor AP-1 did not inhibit the NF-κB DNA binding activity (lane 3). The

competitive inhibition of the DNA binding activity confirmed NF-κB-specific binding.

Functional integrity of radiation-induced activation of NF-κB: To determine whether radiation triggered DNA binding activity of NF-κB is functionally viable and could up-regulate the κB -dependent gene expression, transient transfection assays were performed. MCF-7 cells were transiently transfected with pNF-κB -Luc plasmid construct that expresses the luciferase reporter gene in an NF-κB-dependent manner. It contains four tandem copies of the NF-κB consensus sequence fused to a TATA-like promoter region of herpes simplex virus's thymidine kinase promoter. Functionally active NF-κB specifically binds to the promoter and activates transcription allowing reporter gene to be expressed. Cells transfected with pTAL-Luc vector were used as a negative control as well as to measure the background. A promoter/enhancer less pGL3-basic vector was used as a transfection control. Transfected cells either mock irradiated or exposed to 2 Gy and harvested at 16 h were assayed for luciferase activity. Absence of luciferase activity in cells transfected with pGL3-basic vector and then irradiated confirmed the absence of gene expression due to transfection procedure using cationic lipid reagents. Minimal luciferase activity was observed in cells transfected with the pTAL-Luc control vector. The luciferase activity was first normalized with the minimal levels seen with pTAL-Luc control vector (negative). The induced levels in cells transfected with pNF-κB-Luc plasmid construct were then calculated by comparing the levels seen in mock-irradiated cells. To ensure that the luciferase assay was within the linear range, the standard curve of light-units versus relative enzyme concentration was obtained by making serial dilutions of recombinant luciferase (Promega, Madison, WI) in 1 x lysis buffer with 1 mg/ml BSA. Compared to mock irradiated control, the luciferase activity in cells exposed to 2 Gy was slightly increased at 8h (1.3± 0.07-fold), the earliest time point examined. The activity was increased to its maximal level at 24 h

(2.3 ± 0.06-fold) and reduced at 48 h (1.5 ± 0.09-fold) (Figure 2). Cells exposed to 10 Gy showed only a slight increase at 24 h (1.4 ± 0.07- fold) and remained at the constitutive levels at 8 and 48 h. Similarly, cells transfected with pTAL-Luc control vector remained at the basal levels at all time points examined. These results clearly indicated that induction of NF-κB DNA binding activity seen after 2Gy was functionally active and therefore could initiate activation of NF-κB-dependent gene transcription.

Radiation induces TNF-α expression: If the pro-inflammatory cytokine TNF-α is involved in radiation-triggered autocrine feed-back cycle through membrane associated receptor-mediated mechanism, post-exposure expression followed by secretion of TNF-α should occur. To study whether exposure of MCF-7 cells to radiation could induce TNF-α expression and subsequent secretion, TNF-α level was measured in terms of its bioactivity in the culture medium collected from MCF-7 cells that were either mock irradiated or exposed to 2 or 10 Gy and harvested at 8 and 24 hours. The secreted TNF-α level in the culture supernatant from cells exposed to 2 Gy and harvested at 8 hours showed a 1.9 ± 0.08-fold increase compared to mock-irradiated control. The amount of secreted TNF-α remained at the same level even after 24 hours post radiation (Figure 3). TNF-α bioactivity in culture supernatant of the cells exposed to 10 Gy did not show marked increase. The levels were 1.4 ± 0.1 and 1.2 ± 0.2 -fold at 8 and 24 h, respectively.

TNF-α expression after 2 Gy exposure is mediated by Radiation-triggered NF-κB: To determine the causal relationship of NF-κB activation and etracellular TNF-α synthesis in the culture supernatant, alterations in TNF-α level was measured after blocking NF-κB activation. MCF-7 cells were incubated with NF-κB inhibitor isoheleninm (Calbiochem, NJ) for 6 hours. Isohelenin is a cell-permeable sesquiterpene lactone with anti-inflammatory properties and acts as a highly specific, potent, and irreversible inhibitor of NF-κB activation by preventing IκB

degradation. Intact IκB remain bound to NF-κB and prevent the active NF-κB to translocate into the Nucleus. When NF-κB-dependent transactivation was inhibited, the levels of secreted TNF-α was decreased about 50% and 40% in cells exposed to 2 Gy and harvested at 8 and 24 h, respectively (Figure 3).

TNF-α-dependent second phase activation of NF-κB: First, we examined whether the rapid activation of NF-κB in the irradiated cells was transient or persistent. MCF-7 cells were exposed to 2 or 10 Gy, re-incubated and harvested at 15 min, 3 h, 12 h, 24, 36 and 48 h for EMSA analysis. There was a persistent activation of NF-kB after radiation exposure. However, radiation-induced activation of NF-kB appeared to be bi-phasic. The activation was found to be maximum at 3 h showing a 4.8 ± 0.3 and 3.4 ± 0.8 –fold increase after 2 and 10 Gy, respectively, compared to mock irradiated control. The DNA-binding activity of NF-kB was reduced to the basal level at 12 h (1.1 ± 0.2 –fold after 2 Gy and 1.2 ± 0.1 –fold after 10 Gy). Again at 24 h after irradiation, the DNA-binding activity was started to increase and reached a second maximum at 36h (Figure). Since IR-induced soluble TNF-a levels were elevated in the culture supernatant of MCF-7 cells, and since ectopically added recombinant TNF-a is a known inducer of NF-kB, next we examined whether the secreted TNF-α act as an autocrine inducer for the second phase activation of NF-κB signaling. MCF-7 cells were incubated with TNF-α neutralizing antibody at 8, 12 and 16 h after radiation. If the secreted TNF is responsible for the second phase activation of nF-kB, the blocking of TNF-a with the neutralizing antibody would inhibt the activation seen at 24 and 36 h. Pre-immune IgG was used as the antibody control. In the presence of TNF-α antibody, the 2^{nd} phase activation of NF-κB seen at 24 and 36 h was significantly inhibited, confirming that the secreted TNF-α was responsible for the stimulation of NF-κB activity at later time point (Figure 2.7 A and B).

Bystander Effect

To determine the mechanism of TNF-α mediated bystander effect in the un-irradiated neighboring cells: To study whether TNF-α regulates NF-κB activation in the bystander cells**,** medium from MCF-7 cells that are irradiated and incubated for 24 hours was transferred into the cultures of non-irradiated MCF-7 cells. We found that the DNA-binding activity of NF-κB was increased to 7.2 ± 1.4-fold in the non-irradiated cells as early as 15 minutes compared to the mock-irradiated control (Figure 2.8 A and B). The activation was persistent up to 24 h, the latest time point studied. Similarly the luciferase activity also corroborated the results of DNA binding activity showing an increased functional activation of NF-κB in the un-irradiated bystander cells (Figure 2.8 C) upon transfer of medium from the irradiated cells. To investigate the possibility that the presence of secreted TNF-α in the medium from the irradiated cells may be responsible for the initiation of NF-κB signaling in the non-irradiated cells, we transferred the conditional medium from the irradiated cells after blocking TNF-α by incubating with TNF-α neutralizing antibody for the last 8 hours (i.e. 16 hours after irradiation) prior to adding to the non-irradiated MCF-7 cells. Measure of functional assay showed an induced levels of luciferase activity in the non-irradiated MCF-7 cells at 3 h after the addition of the conditional medium (Figure 2.8 D). Cells at passages 3 were used to start the culture, cell passage 4-8 were used for all the experiments.

Since not all L929 fibroblast cells are TNF-a sensitive and those that are, vary in their degree of sensitivity (Hogan and Vogan, 2000), cellular susceptibility to TNF-a was evaluated using serial dilution of recombinant human TNF-a (rhTNF-a) by WST cytotoxicity assay ( ).

In summary the findings revealed that **(a)** NF-κB DNA-binding activity is triggered in MCF-7 cells after exposure to radiation at clinically relevant doses; **(b)** the radiation-induced activation of NF-κB is bi-phasic, showing 1st maximum level at 3h and the 2nd peak at 24 h; **(c)** the induced NF-κB activation is functionally viable that it could transactivate the κB-dependent downstream genes; **(d)** radiation at clinical doses could stimulate the expression and secretion of TNF-α into the culture medium; **(e)** TNF-α secretion was NF-κB dependent and the radiation-induced rapid activation of NF-κB at 3 h is responsible for the transactivation of TNF-α gene expression; and **(f)** TNF-α mediates the second phase activation of NF-κB through autocrine mechanism. The time relationship between the rapid activation of NF-κB upon radiation exposure, increased TNF-α mRNA expression soon after NF-κB activation, accumulation of TNF-α protein product at later time period, 16 h, NF-κB-dependent TNF-α expression and TNF-α mediated NF-κB activation in the irradiated strongly support the hypothesis that the activation of the transcriptional regulator NF-κB by low LET radiation will lead to positive feed back cycle thereby retain the memory of the initial irradiation insult for an extended period of time and simultaneously could cause the bystander effect.

Figure Legends:

Figure 1: Radiation induced TNF-α production in MCF-7 cells and MM-6 cells. MM-6 cells were used to standardize the method. MCF-7 were either exposed to 2 Gy and 10 Gy or mock irradiated, and then incubated for additional 8 hrs and 24 hrs. TNF-α was determined as described above. The levels of TNF-α expression in cells exposed to 2 Gy or 10 Gy radiation were normalized to those with exposure to mock radiation. The data shown represent mean ± SD of three independent experiments.

Figure 2: (A) Dose- and time-dependent NF-κB DNA binding activation in the neighboring non-irradiated MCF-7 cells. Medium from MCF-7 cells that are irradiated and incubated for 24 hours is transferred into the cultures of non-irradiated MCF-7 cells. After 15 minutes and 24 hours, non-irradiated cells were harvested and EMSA was performed to examine NF-κB activation. The densities of bands were normalized to mock control **(B).** The data shown are the mean ± SD from three independent experiments. **(C)** Intact transactivation property of NF-κB in the neighboring non-irradiated MCF-7 cells. Medium from MCF-7 cells that are irradiated and incubated for 24 hours is transferred into the cultures of non-irradiated MCF-7 cells transfected with pNF-κB-Luc or pTAL-Luc control. After 15 minutes, 3 hours, 12 hours and 24 hours, non-irradiated cells were harvested and luciferase activity was measured. Data shown represent mean ± SD of three independent experiments. **(D)** TNF-α mediated stimulation of NF-κB in non-irradiated MCF-7 cells. Medium of irradiated MCF-7 cells was incubated with TNF-α neutralizing antibody for 8 hours and transferred to the non-irradiated MCF-7 cells transfected with p NF-κB-Luc or pTAL-Luc control. After 15 minutes, 3 hours, 12 hours and 24 hours, non-irradiated cells were harvested and luciferase activity was measured. Data shown are the mean ± SD of three independent experiments.

Figure 3: (A) EMSA showing radiation-induced NF-κB DNA-binding activity. Specific bands are indicated by arrowhead. Relative unbound free probe indicates equal gel loading. **(B)** Competition experiment showing specificity of NF-κB DNA-binding activity. Cells either mock-irradiated (Lane 2) or exposed to 2 Gy (lanes 1, 3, 4 & 5) were incubated with non-homologous competitor AP-1 or increasing concentrations of (2.5 molar excess, lane 4 and 25 molar excess, lane 5) homologous unlabelled competitor. **(C)** Kinetics of NF-κB DNA-binding activity in MCF-7 cells exposed to 2 Gy or 10 Gy. The increase in stimulation was calculated by taking the

ratio of the optical densities of the induced level of NF-κB activity to that of the constitutive level (0 Gy) at each incubation time from three independent experiments (mean ± SD).

Figure 2.4: Transactivation property of NF-κB upon 2 Gy and 10 Gy exposures. The MCF-7 cells were transfected with an empty vector (B) or a vector containing an NF-κB-luciferase construct (A). Luciferase activity was measured by a dual luciferase assay. Data shown represent mean ±SD of three independent experiments.

Figure 2.5: Radiation induced TNF-α production in MCF-7 cells and MM-6 cells. MM-6 cells were used to standardize the method. MCF-7 were either exposed to 2 Gy and 10 Gy or mock irradiated, and then incubated for additional 8 hrs and 24 hrs. TNF-α was determined as described above. The TNF-α quantity of cells exposed to 2 Gy or 10 Gy radiation were normalized to those with exposure to mock radiation. The data shown represent mean ± SD of three independent experiments.

Figure 2.6: Radiation induced TNF-α production in MCF-7cells through NF-κB regulation. MCF-7 were exposed to 2 Gy, and then incubated with isohelenin for 6 hours before secreted TNF-α level was determined. The TNF-α level after radiation alone exposed cells were considered 100 percent induction. The data shown represent mean ± SD of three independent experiments.

Figure 2.7: TNF-α-dependent 2nd-phase activation of NF-κB. EMSA analysis was performed to determine the activation of NF-κB in the nuclear extracts of cells that were exposed to mock or 2 Gy radiation and harvested at 24 hours. To study the role of TNF-α in this process, the cultures were added with TNF-α antibody after 8, 12 and 16hours post irradiation, then harvested at 24h post irradiation **(A)**. The densities of bands were normalized to those with mock radiation **(B)**, lane 1 is control, and lane 2 is activation of NF-κB in MCF-7 cells after 2 Gy radiation

exposures, lane 3, 4, 5 represent that activation of NF-κB in MCF-7 cells after 2 Gy radiation exposures, then incubated with TNF-α antibody for 16, 12 and 8 hours. The data shown are the mean ± SD from three independent experiments.

Figure 2.8: (A) Dose- and time-dependent NF-κB DNA binding activation in the neighboring non-irradiated MCF-7 cells. Medium from MCF-7 cells that are irradiated and incubated for 24 hours is transferred into the cultures of non-irradiated MCF-7 cells. After 15 minutes and 24 hours, non-irradiated cells were harvested and EMSA was performed to examine NF-κB activation. The densities of bands were normalized to mock control **(B).** The data shown are the mean ± SD from three independent experiments. **(C)** Intact transactivation property of NF-κB in the neighboring non-irradiated MCF-7 cells. Medium from MCF-7 cells that are irradiated and incubated for 24 hours is transferred into the cultures of non-irradiated MCF-7 cells transfected with pNF-κB-Luc or pTAL-Luc control. After 15 minutes, 3 hours, 12 hours and 24 hours, non-irradiated cells were harvested and luciferase activity was measured. Data shown represent mean ± SD of three independent experiments. **(D)** TNF-α mediated stimulation of NF-κB in non-irradiated MCF-7 cells. Medium of irradiated MCF-7 cells was incubated with TNF-α neutralizing antibody for 8 hours and transferred to the non-irradiated MCF-7 cells transfected with p NF-κB-Luc or pTAL-Luc control. After 15 minutes, 3 hours, 12 hours and 24 hours, non-irradiated cells were harvested and luciferase activity was measured. Data shown are the mean ± SD of three independent experiments.